Proteomic evidence of astrocytic dysfunction in the olfactory bulb of depressed suicides

Reza Rahimian[1,2†], Kelly Perlman[1,3†], Gohar Fakhfouri[4†], Refilwe Mpai[1,3], Vincent R. Richard[5], Christa Hercher[1,3], Lucy Penney[4], Maria Antonietta Davoli[1,2], Corina Nagy[1,2,3], René P. Zahedi[6,7,8,9], Christoph H. Borchers[5,10,11,12], Bruno Giros[4], Gustavo Turecki[1,2,3], Naguib Mechawar[1,2,3*]

[1]McGill Group for Suicide Studies, Douglas Mental Health University Institute, Verdun, QC, Canada.
[2]Department of Psychiatry, McGill University, Montreal, QC, Canada.
[3]Integrated Program in Neuroscience, McGill University, Montreal, QC, Canada.
[4]Department of Psychiatry, Douglas Hospital, McGill University; Montreal, QC, Canada
[5]Segal Cancer Proteomics Centre, Lady Davis Institute for Medical Research, Jewish General Hospital, McGill University, Montréal, QC, Canada.
[6]Department of Internal Medicine, University of Manitoba, Winnipeg, MB, Canada.
[7]Manitoba Centre for Proteomics and Systems Biology, University of Manitoba, Winnipeg, MB, Canada.
[8]Department of Biochemistry and Medical Genetics, University of Manitoba, Winnipeg, MB, Canada.
[9]CancerCare Manitoba Research Institute, Winnipeg, MB, Canada.
[10]Gerald Bronfman Department of Oncology, McGill University, Montréal, Québec, Canada
[11]Department of Pathology, McGill University, Montréal, QC, Canada
[12] Department of Experimental Medicine, McGill University, Montreal, QC, Canada

† These authors contributed equally

[*]Corresponding author:
Naguib Mechawar, PhD
Douglas Mental Health University Institute, 6875 Boulevard LaSalle, Montréal, Quebec, Canada, H4H 1R3
e-mail: naguib.mechawar@mcgill.ca

Abstract

Brain regions involved in olfaction, including the olfactory bulb, have been implicated in the etiology of major depression mainly on the basis of rodent models of the illness. To explore more directly the molecular features of the olfactory bulb (OB) in major depression, a global comparative proteome analysis was carried out with human OB samples from 12 middle-aged male depressed suicides and 12 matched controls. Cases displayed a significant reduction in astrocytic proteins. Furthermore, using RNA-fluorescence *in-situ* hybridization, we observed a decrease in the percentage of ALDH1L1+ cells expressing canonical astrocytic markers including *ALDOC*, *NFIA*, *GJA1 (connexin 43)* and *SLC1A3 (EAAT1)*. These results are consistent with previous reports of downregulated astrocytic marker expression in other brain regions in depressed suicides. We also conducted a comparative phosphoproteomic analysis of OB samples and found a dysregulation of proteins involved in neuronal and astrocytic functions. To determine whether OB astrocytic abnormalities can be observed in an animal model of depression, we also performed proteomics on the OB of socially defeated mice. Cell-type specific analysis revealed that in socially defeated animals, the most striking OB protein alterations were associated with oligodendrocyte-lineage cells rather than with astrocytes, highlighting an important species difference. Overall, this study further highlights cerebral astrocytic abnormalities as a consistent feature of depression and suicide in humans, and suggests that animal models of depression may not display all cellular and molecular features of depression, at least not in the OB.

Keywords: Olfactory bulb (OB); Major depressive disorder; Limbic system; Proteomic; Phospho-proteomic; Astrocyte, Oligodendrocyte

INTRODUCTION

The olfactory bulb (OB) is part of the limbic system, a group of brain structures involved in motivation, emotion, learning, and memory (Milardi et al., 2017). The OB transmits olfactory information to other limbic areas, including the amygdala, hippocampus, and the anterior cingulate cortex (Milardi et al., 2017). The OB is also one of the two main brain regions, in rodents at least, in which neurogenesis occurs in adulthood (Maheu et al., 2015; Mechawar et al., 2004). Different brain regions that participate in the processing of olfactory information have been implicated in depression (Croy and Hummel, 2017; Kohli et al., 2016; Rottstaedt et al., 2018). In rodents, bilateral olfactory bulbectomy results in a depression-like phenotype and chronic antidepressant administration can rescue the associated behavioral and physiological changes (Kelly et al., 1997; Song and Leonard, 2005). As such, bulbectomized rats have been used as an animal model of depression (Song and Leonard, 2005). Interestingly, humans with OB aplasia (congenital anosmia) have higher rates of depressive symptoms (Croy et al., 2012; Rottstaedt et al., 2018), and patients with depression have been reported to display decreased olfactory sensitivity and discrimination (Lombion-Pouthier et al., 2006; Negoias et al., 2010). Moreover, structural MRI has revealed a smaller OB volume in depressed patients compared to healthy controls (Negoias et al., 2010). Given the highly evolutionarily conserved OB-limbic circuitry, and the resulting functional connections between the olfactory, salience, and emotional brain networks (Croy and Hummel, 2017; Kohli et al., 2016; Rottstaedt et al., 2018; Takahashi et al., 2016), these observations strengthen the hypothesis that depression is associated with impaired OB structure and function. The underlying cellular and molecular changes, however, remain largely unexplored, especially in humans. To examine the molecular alterations occurring in the OB in major depressive disorder (MDD), the present study aimed at performing the first

unbiased global proteome and phosphoproteome analysis of post-mortem OB samples from depressed suicides and matched healthy controls. We found that astrocytic proteins were significantly enriched among the differentially expressed proteins (DEP) between cases and controls. RNA-fluorescence *in-situ* hybridization (FISH), revealed changes at the RNA level that correlated with the decreased protein levels identified using proteomics. In contrast, analyzing OB from socially defeated mice vs controls showed that oligodendrocyte (OL)-lineage – rather than astrocytic – cell markers were significantly altered. Altogether, these results further highlight the occurrence of cerebral astrocytic dysfunctions in depression and point to a critical difference in the OB proteome of depressed patients and socially defeated mice.

MATERIAL AND METHODS

Human OB samples

Post-mortem OB samples from depressed suicides and matched controls were obtained from the Douglas-Bell Canada Brain Bank (Montreal, Canada). The Douglas-Bell Canada Brain Bank maintains a collaboration with the Quebec Coroner's Office, and all phenotypic information was obtained via standardized psychological autopsies, with informed consent provided by the next of kin (Dumais et al., 2005). Either presence or suspected presence of any neurological or neurodegenerative disorders based on clinical files was an exclusion criterion for this study. Information from the Coroner's office, medical records, social services records, and toxicological analysis were complemented with proxy-based interviews with one or more informants best acquainted with the donor. Clinical vignettes realized by combining all this information were evaluated by a panel of clinicians who, using Diagnostic and Statistical Manual

of Mental Disorders (DSM-IV) criteria, to establish a diagnosis (Dumais et al., 2005; Tanti et al., 2022).

Two distinct sets of fresh-frozen OB samples from MDD patients and matched controls were used in this study: one for proteomic and phosphoproteomic analyses (12 and 9 samples/group, respectively) and the other for RNA-fluorescent *in situ* hybridization experiment (5 and 3 samples/group, respectively). Although the same OB lysate was used for proteomic and phosphoproteomic analyses, phosphoprotein enrichments were only successfully done in 9 control and 9 MDD samples. Group characteristics, including age, post-mortem interval (PMI), tissue pH, substance dependence, and medication, are presented in Supplementary Tables 1 and 2.

Chronic social defeat stress and mouse OB samples

Animal experiments were conducted with the approval of the Douglas Animal Care Committee. Male C57BL/6 mice were subjected to a social defeat paradigm, consisting of a daily 5-minute defeat with a different CD-1 aggressor mouse on each of 10 consecutive days (Golden et al., 2011) (all details are provided in the Supplementary Methods). Twenty-four hours following the last behavioral test, socially defeated and control mice were euthanized, the OB pairs were extracted on an ice-cold metal surface, snap frozen and kept at -80˚C for proteomics analysis. For the social defeated group, only susceptible mice consistently displaying susceptibility throughout the behavioral tests (Open Field, Social Interaction and Elevated Plus Maze; all details are provided in the Supplementary Methods) following the chronic stress paradigm were chosen. Every two pairs of OBs were pooled to serve as a single biological replicate.

Proteomic and phosphoproteomic experiments and analyses

For both human and mouse samples, proteins were extracted from whole frozen OBs in tissue lysis buffer containing 5% SDS (Fisher Chemical), 100 mM TRIS (Fisher BioReagents™) pH 8.5 supplemented with PhosStop phosphatase inhibitor as well as cOmplete™ mini protease inhibitor cocktail (Roche). Samples were subjected to probe-based sonication using a Thermo Sonic Dismembrator and subsequently heated at 95° C for 10 minutes. A portion of the sample (less than 5% by volume) was reserved for total protein quantitation by BCA assay (Thermo/Pierce). Disulfide bonds were reduced and alkylated with 20 mM TCEP and 25 mM iodoacetamide. 50 µg of protein per sample was digested with trypsin (Promega) overnight at 37°C using S-TRAP micro cartridges (Protifi LLC,). Peptide-containing samples were desalted using Waters Oasis HLB SPE cartridges. 10% of the sample was reserved for measurement of the total proteome, and the remainder was used for Fe-(III)-NTA based immobilized metal affinity chromatography (IMAC)-based automated phosphopeptide enrichment using an Agilent Bravo liquid handling robot and Agilent AssayMap IMAC cartridges (Beck et al., 2017; Burkhart et al., 2012; Gonczarowska-Jorge et al., 2017). Samples were analyzed by nano Liquid Chromatography with tandem mass spectrometry (LC-MS/MS) by data dependent acquisition (DDA) using an Easy nLC 1200 coupled with a Q Exactive Plus mass spectrometer (Thermo Fisher Scientific).

Samples were first loaded onto a pre-column (Acclaim PepMap 100 C18, 3 µm particle size, 75 µm inner diameter x 2 cm length) in 0.1% formic acid (buffer A). Peptides were then separated using either a 100-min binary gradient for total ranging from 3-40% B (84% acetonitrile, 0.1% formic acid) on the analytical column (Acclaim PepMap 100 C18, 2 µm particle size, 75 µm

inner diameter x 25 cm length) at 300 nL/min. MS spectra were acquired from m/z 350-1,500 at a resolution of 70,000, with an automatic gain control (AGC) target of 1 x 106 ions and a maximum injection time of 50 ms. The 15 most intense ions (charge states +2 to +4) were isolated with a window of m/z 1.2, an AGC target of 2 x 104 and a maximum injection time of 64 ms and fragmented using a normalized higher-energy collisional dissociation (HCD) energy of 28. MS/MS spectra were acquired at a resolution of 17,500 and the dynamic exclusion was set to 30 s. DDA MS raw data was processed with Proteome Discoverer 2.5 (Thermo Scientific) and searched using Sequest HT against a FASTA file containing all reviewed protein sequences of the canonical human proteome without isoforms downloaded from Uniprot. The enzyme specificity was set to trypsin with a maximum of 2 missed cleavages. Carbamidomethylation of cysteine was set as static modification and methionine oxidation as variable modification. The precursor ion mass tolerance was set to 10 ppm, and the product ion mass tolerance was set to 0.02 Da. The percolator node was used, and the data was filtered using a false discovery rate (FDR) cut-off of 1% at both the peptide and protein level. The Minora feature detector node of Proteome Discoverer was used for precursor-based label free quantitation (Beck et al., 2017; Burkhart et al., 2012; Gonczarowska-Jorge et al., 2017). Only peptides that are unique to a protein were used for quantitation. In cases where a protein was not found in a particular sample, we imputed the missing areas using Low Abundance Resampling, an algorithm that randomly uses an area value from the lowest 5% of those detected (Gonczarowska-Jorge et al., 2017).

For human samples, proteins or phosphoprotein modifications that were not detected in at least 50% of subjects in both cases and controls were removed. This conservative approach was chosen to increase the robustness of our results given the small sample size, as it ensured that

each protein had absolute quantities that were as representative of the group as possible (i.e., no imputation required) without excluding too many proteins. For mouse samples, we elected to remove any protein that was not detected in at least 1/3 of the samples from both groups, since each sample was derived from the combination of 2 OBs and inter-subject variability was lower (6 OBs in Control and 6 OBs in social defeated mice). The underlying data structure was visualized using PCA and Grubb's test was used to identify outliers for removal. Differentially expressed proteins (DEP), referring to proteins whose abundances are significantly different between cases and controls, were computed with t-tests that have "background" adjusted p-values which means that a weighting factor is applied to the p-values that takes into account the distribution of ratios for all other proteins as well as the protein abundances themselves (Navarro et al., 2014). P-values were corrected for multiple comparisons with the Benjamini-Hochberg method. This background t-test is designed to fulfill the assumption of data normality as it handles data such that the variance is constant for the reference points of the background. All downstream analyses and data visualizations were conducted in R. Gene ontology and pathway enrichment analyses were conducted with the clusterProfiler package. DEPs were compared with the literature using the DisGeNet database and assessed for overlap between our DEPs and genes that were established to be differentially expressed in the following conditions: Mental Depression (CUI: C0011570), Unipolar Depression (CUI: C0041696), Endogenous depression(CUI: C0011573), Severe depression (CUI: C0588008), Depression and Suicide (CUI: C1524032), clinical depression (CUI: C2362914), Major Depressive Disorder (CUI: C1269683), Major depression (CUI: C1269683), provided that the gda score was greater than 0.01. Over enrichment of cell types based on DEPs was calculated by comparing published sets of gene lists and using fisher's exact test to look for statistically significant overabundance. The list of genes

for each major cell type was formed by taking the union of the markers from the McKenzie et al. (2018) and Qiu et al. (2021), with corresponding MarkerPen tool, plus genes selected to complete the cell type categories which were previously deemed insufficient, primary the OLs.

Fluorescence *in situ* hybridization

Frozen OBs were cut dorsoventrally with a cryostat and 10 µm-thick sections were collected on Superfrost charged slides. *In situ* hybridization was performed using Advanced Cell Diagnostics RNAscope® probes and reagents following the manufacturer's instructions (Reemst et al., 2022). Sections were first fixed in cold 10% neutral buffered formalin for 15 min, dehydrated by increasing gradient of ethanol baths, and air-dried for 5 min. Endogenous peroxidase activity was quenched with hydrogen peroxide for 10 min followed by protease digestion for 30 min at room temperature (Tanti et al., 2022). The following probes were then hybridized for 2 h at 40 °C in a humidity-controlled oven: Hs-ALDH1L1 (ACDbio, REF;438881), Hs-ALDOC (ACDbio, REF;407031), Hs-GJA1(ACDbio, REF;444281), Hs-NFIA (ACDbio, REF;442781) and Hs-SLC1A3 (ACDbio, REF;461081). Amplifiers were added using the AMP reagents and the signal visualized through probe-specific HRP-based detection by tyramide signal amplification (TSA, ACDbio) with Opal dyes (Opal 520 and Opal 570; Perkin Elmer) diluted 1:900. In order to eliminate endogenous autofluorescence from lipofuscin and cellular debris, sections were incubated with TrueBlack (Biotium, Cat; 23007) for 30 seconds. Slides were then cover slipped with Vectashield mounting medium with 4′,6-diamidino-2-phenylindole (DAPI) for nuclear staining (Vector Laboratories, H-1800) and kept at 4 °C until imaging. Both positive and negative controls provided by the supplier (ACDbio) were used on separate sections to confirm signal specificity. The slides were imaged at 20X magnification using the Olympus

VS120 virtual slide scanner and the scans were transferred to QuPath (v.0.3.0) for further analysis. OB area (whole section) was demarcated manually and QuPath was employed for automated cell detection based on DAPI staining and RNAscope signal quantification. For each probe, only cells bearing three or more fluorescent puncta were counted as positively labeled.

Statistical analysis

Values are presented as mean ± SEM and GraphPad Prism (v8) was employed to perform statistical analyses. For animal studies and FISH experiments, unpaired Student *t* tests were used to compare different behavioral parameters and quantifications, respectively. For FISH quantifications, double- labeled astrocytes were assessed using QuPath (v0.3.2) and reported as a percentage of total astrocytes ($ALDH1L1^{+}$). Proteomic and phosphoproteomic analyses were conducted as described in the Supplementary methods. $p < 0.05$ was set as the threshold for statistical significance in all analyses.

RESULTS

Altered expression of canonical astrocyte proteins in OB of depressed suicides

We identified 189 DEPs (with corrected $p<0.05$ for group differences) between cases and controls, which was narrowed down to 145 proteins when using a 2-sigma fold change cut-off (Figure 1A). Gene ontology and gene enrichment analyses suggested that the DEPs are involved in biological processes such as complement and coagulation cascades (e.g., C5, C3, F2, PLG, C4BPA, CFH, CFB), phospholipid biosynthesis (e.g., PIGS, LPCAT2, APOA1, APOA2), and extracellular matrix (ECM) organizations/interactions (e.g., LUM, MFAP4, BGN, TNXB) (Figure 1B-C). Among ECM-related proteins, we observed a decrease in glycoprotein CD44, a protein highly expressed in astrocytes, in the OB of depressed suicides. This cell surface receptor interacts with the ECM and has been found previously to be downregulated in the CSF of suicide attempters (Ventorp et al., 2016). The CD44 gene has been identified in brain GWAS studies as a possible risk gene for suicidal behavior (Ventorp et al., 2016). Given the scarcity of molecular OB research in depression, we sought to assess the extent to which the list of DEPs overlapped with differentially expressed genes reported in the literature for other brain regions in humans. To this end, we used the DisGeNeT database and considered the differentially expressed genes that were common to studies of depressive disorders. We then interrogated the overlap (i.e., intersection) of those genes with the DEPs identified in the current study and found 34 overlapping candidates from our initial total list of 189 proteins (Figure 1D). These 34 candidates included genes involved in the complement cascade, lipid metabolism, and oxidative stress. Since the proteomics analyses were performed on bulk OB tissue, we examined whether the DEP list would suggest any cell type specificity to the alterations. We assessed the overlap between broad cell type specific marker genes (astrocyte, endothelial, microglial, OL-lineage,

and neuronal) provided in Supplementary Table 3, constructed as described in the Methods section. We applied hypergeometric tests on this list to determine cell type enrichment and found that the only cell type that was significantly enriched was the astrocyte (astrocyte, p = 0.00594; endothelial, p = 0.0881; microglia, p = 0.0920; OL-lineage, p = 0.325; neuron, p = 0.9998; Figure 1E). Canonical markers GFAP (p = 0.00128) and SLC1A3 (p = 0.0174) - a glial high affinity glutamate transporter - were among the markers significantly downregulated in depressed suicide OBs in proteomic analysis while astrocyte-specific markers ALDH1L1, ALDOC, NFIA and GJA1 showed a downregulation trend (Figure 2A). To confirm these observations in situ, at the transcriptional level, with a highly sensitive method, we carried out multiplexed fluorescence in situ hybridization (FISH; RNAScope®) to assess canonical astrocytic marker transcripts. We used the pan-astrocytic marker ALDH1L1, and counted positive cells as cells that expressed both the target transcript and ALDH1L1. These experiments confirmed that ALDOC, SLC1A3 (EAAT1), GJA1 (Connexin 43) and NFIA are primarily expressed in human OB astrocytes (Supplemental Figure 1). Furthermore, the number of ALDH1L1-positive cells was not significantly different between groups (p = 0.1406). However, the number of astrocytes expressing ALDOC (p = 0.0272), GJA1 (p = 0.031), NFIA (p = 0.007) and SLC1A3 (p = 0.024) were significantly reduced in the OB of depressed suicides compared to controls (Figure2B-F). As ALDOC is a glycolytic enzyme, its downregulation in depression can be related to the reduction of astrocytic glutamate transporters such as SLC1A3, which was also observed in the OB of cases. According to the astrocyte-neuron lactate-shuttle hypothesis, astrocytes upregulate glycolysis to produce lactate for neurons when glutamate is taken up from the synapse (O'Leary and Mechawar, 2021; Pellerin and Magistretti, 1994; Zhao et al., 2016).

We then accessed a single nucleus RNA sequencing (snRNA-seq) dataset recently generated by our group with human dorsolateral PFC (dlPFC) from depressed suicides and control adult males (Maitra et al., 2023) to compare the differentially expressed genes in its astrocyte clusters to our proteome results. Despite differences in brain regions, we found overlapping genes between the astrocyte 1 dlPFC cluster from the Maitra et al. study (in a re-analysis of the male data from Nagy et al., 2020) and the proteomics data presented here, with 8 out of 9 candidates displaying a downregulation trend compared to controls, according to log fold change (Supplemental Table 4) which indicates a concordance between RNA and protein changes (Maitra et al., 2023; Nagy et al., 2020). Some of these proteins, such as AQP1, MT1X and S1PR1, are highly expressed by astrocytes, and elicit crucial roles in homeostatic and immune-related functions. Namely, S1PR1 is implicated in proliferation and trafficking of immune cells (Rothhammer et al., 2017). By generating high levels of antioxidants including metallothionein-I (MT1X), astrocytes play a key role in offsetting oxidative stress associated with inflammation (Waller et al., 2018).

We then verified that these depression-associated changes in OB astrocytic proteins were not driven by confounders such as child abuse history and antidepressant treatment. As illustrated in Supplemental Figure 2, no significant relationship was found between protein quantities and either of these potential confounders using the Mann-Whitney U-Test (child abuse (CA): ALDOC, p = 0.2101; ALDH1L1, p = 0.3881; GFAP, p = 0.1826; GJA1, p = 0.3091; NFIA, p = 0.7941; SLC1A3, p = 0.1573. Antidepressant treatment: ALDOC, p = 0. 0.1085; ALDH1L1, p = 0. 0.5584; GFAP, p = 0. 0.3472; GJA1, p = 1.0000; NFIA, p = 0.3472; SLC1A3, p = 0.1553).

Dysregulation of phosphoproteins in the OB of depressed suicides

The phosphoproteome is more dynamic than the proteome, thus we expected some discordance with the proteome results. We found 57 differentially abundant phosphopeptides, corresponding to 50 individual proteins, all of which met the 2-sigma fold change cut-off (Figure 3A). Gene ontology indicated that the corresponding proteins of the differentially abundant phosphopeptides are involved in biological processes such as cell cycle (e.g., CCSAP, CDK14, SPTBN1), synaptic vesicle cycle (e.g., AMPH, SYN1, SYN2, PPFIA2), and phosphorus metabolic processes (e.g., PNPO, ATP2B4, SLC4A1) (Figure 3B). We assessed overlap between this list of 57 phosphopeptides and DisGeNET differentially expressed genes for depression and found 10 overlapping candidates (Figure 3C). We performed the same cell-type specific hypergeometric tests as in the proteomic analysis and that both neurons (p = 0.0125), and astrocytes (p = 0.0281) were significantly enriched, with neurons having the highest enrichment score (endothelial, p = 0.665; microglia, p = 1.000; OL-lineage, p = 0.733; Figure 3D).

We also examined the relationship between the proteome and phosphoproteome differential abundance. As listed in Supplemental Table 5, there are nine proteins overlapping between the two analyses, including GFAP and AQP1, which are fairly specific to astrocytes in the adult human brain. SLC1A4 had two differentially abundant phosphopeptides, both upregulated, as was observed for the protein. In fact, the regulation direction was found to be consistent for all but one protein (ARHGEF6). For instance, both GFAP protein and a GFAP phosphopeptide were downregulated in cases compared to controls and was identified in the DisGeNET dataset as well.

Dysregulation of oligodendrocyte proteins in OB of socially defeated mice

To examine whether human OB findings could be observed in a mouse model of depression, we performed the same proteomics analyses with socially defeated mice and controls. Proteins were extracted from 3 control and 3 socially-defeated OB pairs (each sample was derived from 2 OBs, yielding 6 subjects per group in total). As presented in the Methods section, only susceptible mice consistently showing susceptibility throughout the behavioral tests (Open Field, Social Interaction and Elevated Plus Maze) following chronic stress were chosen for proteomic analyses (Figure 4A-C). The analysis revealed 261 significantly DEPs, 193 of which also met the fold change cut-off (Figure 4D). Gene ontology analyses suggested that these proteins are involved in functions such as post-transcriptional regulation of gene expression (e.g. Pum1, Nemf, Gcn1), axon guidance (e.g. Unc5b, Lama1), and neurogenesis (e.g. Frmd7, Ndel1, Cit) (Figure 4E). We found 35 DEPs overlapping with the DisGeNET database, indicating overlap with genes previously implicated in MDD (Figure 4F). Strikingly, we found a different pattern of cell type enrichment in the DEPs, as the only cell type reaching our significance cut-off was OL-lineage cells (p = 0.0453), with endothelial cells showing a trend (endothelial p = 0.0679, astrocyte p = 0.733, microglia p = 0.627, neuronal p = 0.375) (Figure 4G). For instance, plp1 (p = 0.0106), anln (p = 0.0299), apc (p = 0.000765), ptgds (p = 0.00000309) and tf (p = 0.000000189) were among the strongly dysregulated OL markers in socially defeated mice. These genes have all been implicated in the process of myelination, with plp1 being the most abundant protein in myelin of the central nervous system (Jahn et al., 2009).

We then conducted a species comparison and found 20 overlapping DEPs including cat (involved in oxidative stress), apoa1 (involved in lipid metabolism), as well as ncs1 (neuronal calcium sensing). According to log fold change, 14 of these 20 proteins were regulated in the same direction in both species (Supplemental Table 6).

DISCUSSION

This is the first study to compare adult OB proteomic and phosphoproteomic profiles between depressed suicides and matched controls. We observed that depressed suicides presented DEPs that are enriched in astrocytes, which led us to explore whether these findings were reflective of changes in the astrocyte population. While the percentage of ALDH1L1^{+} astrocytes remained similar between depressed suicides and controls, the percentages of astrocytes expressing the canonical markers ALDOC, GJA1, NFIA, and SLC1A3 were significantly reduced in the OB of cases. In addition to these cell type-enriched changes, we also found that there was a substantial overlap between depression-associated dysregulated OB proteins and genes previously implicated in depression across other brain regions. Moreover, parallel analyses conducted with a mouse model of depression revealed that, in contrast to humans, differentially expressed proteins in the OB of socially stressed animals were enriched in proteins associated with OLs.

Astrocytic abnormalities have been consistently implicated in depression and suicide (Torres-Platas et al., 2016), with reported downregulations of astrocyte-specific genes, decreased immunoreactivity to astrocyte-canonical markers, and reduced blood vessel coverage by astrocytic endfeet in postmortem brain samples from MDD patients (Rajkowska et al., 2013). Surprisingly, and despite neuroimaging and psychometric studies implicating the OB in depression, this major limbic region had never been examined at the cellular/molecular level in MDD patients. Our results provide the first evidence that in MDD and suicide, astrocytic abnormalities are present in the OB, in agreement with our previous reports of astrocytic abnormalities in other cortico-limbic brain regions of depressed suicides (O'Leary et al., 2021; O'Leary and Mechawar, 2021; Torres-Platas et al., 2016; Xiong et al., 2019), as well as with

independent animal studies having implicated astrocytes in depression-like behavior (Abbink et al., 2020; Codeluppi et al., 2021; Du Preez et al., 2021; Rurak et al., 2021; Simard et al., 2018).

Depression-associated changes in astrocytic numbers and functions could result from a variety factors, such as chronic glucocorticoid exposure or altered neurotrophic or neurotransmitter signaling (Rajkowska and Miguel-Hidalgo, 2007). The current study indirectly implicates the role of astrocytic transcription factor NFIA, which has been reported to regulate astrocyte morphology and function in the rodent hippocampus (Huang et al., 2020). In addition, these authors found that NFIA-deficient astrocytes or simply hypo-functional NFIA can impair neuron-astrocyte communication *in vitro* (Huang et al., 2020). Interestingly, within 5 days, transient NFIA expression *in vitro* activates glial potential in human pluripotent stem cells, transforming them into astrocytes upon exposure to glial-promoting factors. These NFIA-induced astrocytes not only foster synaptogenesis but also exhibit neuroprotective properties (Tchieu et al., 2019). We can speculate that the reduction in NFIA measured here in the OB of depressed suicides impairs the morpho-functional properties of astrocytes, having in turn an impact on OB volume and olfactory sensitivity, which have both been documented in depressed patients (Negoias et al., 2010; Pause et al., 2001). A smaller OB volume has been associated with higher rates of depressive episodes and with decreased signaling with other limbic areas (Athanassi et al., 2021; Croy and Hummel, 2017). Altered olfaction in depression has been also hypothesized to be linked to a decreased receptor turnover rate in the olfactory epithelium (Athanassi et al., 2021; Croy and Hummel, 2017). Our finding of astrocytic disruptions in the OB of depressed suicides might be associated with this phenomenon and contribute directly to

changes in perception, since mature OB astrocytes, at least in mice, are required for normal physiological sensory processing (Ung et al., 2021).

To better understand the effects of protein regulation in depression, our study also compared differentially phosphorylated proteins in OB samples from depressed suicides compared to matched controls. Changes in phosphorylation almost always reflects a change in protein activity, although many such modifications remain uncharacterized (Ardito et al., 2017). In agreement with our DEP analysis, which highlighted an enrichment of astrocyte proteins in the OB of depressed suicides, the phosphoproteomic analysis revealed a corresponding enrichment in differentially phosphorylated astrocytic proteins. Interestingly, it also revealed enrichment in differentially phosphorylated neuronal proteins. It is well established that astrocytes are an essential component of synapses, regulating both synaptic and circuit plasticity and function (Perez-Catalan et al., 2021). In consequence, the astrocytic dysregulation suggested by our study may impact neuronal functions at various levels, including through post-translational modifications of synaptic proteins. Furthermore, given the converging evidence implicating alterations in synaptic density, synapse microenvironment, and synaptic vesicle release (Duman et al., 2016; Holmes et al., 2019; Ren and Guo, 2021) in depression, it is not surprising that some of our most prominent differentially expressed phosphoproteins are localized at the synapse. This can be illustrated by synapsin (SYN) 1 and 2, which were found to be significantly different between depressed suicides and controls. Synapsins are ubiquitous phosphoproteins on synaptic vesicles, where they regulate the trafficking of vesicles in nerve terminals, a critical parameter in short-term synaptic plasticity (Sun et al., 2006). A previous study of depression in postmortem dlPFC from males and females pointed to synaptic function as the main biological process

associated with differentially expressed phosphoproteins (Martins-de-Souza et al., 2012). Interestingly, 10 out of the 50 phosphoproteins we found to be differentially expressed were similarly differentially expressed in the latter study, despite the regional difference. In our results, SYN 1 was one of the top differentially expressed phosphoproteins with three significantly downregulated phosphopeptides, indicating hypophosphorylation of SYN 1 in depressed suicides compared to controls. This finding was mirrored by significantly downregulated SYN 1 phosphopetides in Martins-de-Souza et al. (2012) (Martins-de-Souza et al., 2012). The sizable overlap between these two studies further strengthens the evidence for post-translational modifications occurring at the synapse in depression.

We then conducted the same OB proteomic analysis in a mouse model of depressive-like behavior. These experiments in the social defeat mouse model indicated that the enriched astrocyte signature observed in depressed suicides is not shared by chronically stressed mice, possibly highlighting a limitation of this model which recapitulates many of the molecular signatures of depression in regions such as the medial prefrontal cortex (mPFC) and nucleus accumbens (Scarpa et al., 2020). However, our observation adds to the extensive breadth of evidence supporting OL lineage abnormalities that have been reported in post-mortem and animal model studies of depression (Liu et al., 2012; Makinodan et al., 2012; Nagy et al., 2020; Rahimian et al., 2022). In a study of chronic social defeat stress, decreases in myelin proteins were observed in the nucleus accumbens and mPFC, with the mPFC also displaying thinner myelin and decreased internode length (Bonnefil et al., 2019). In another study, this model led long lasting reductions of OL precursor cells (OPC), abnormal differentiation rates of OPC to OLs, and extensive hypomyelination (Kokkosis et al., 2022). In fact, these findings are not limited to social defeat stress, as myelin-related molecular and ultrastructural changes have been

reported in several models of stress including social isolation and chronic variable stress (Bonnefil et al., 2019; Liu et al., 2012; Rahimian et al., 2022). While our OL enrichment findings may point to differences in myelin content or regulation in socially defeated mice, further experiments are needed to better understand the biological significance of these results. It is also a possibility that discordance in results might reflect differences in OB cellular composition between species. In summary, while there was overlap between human and mouse DEPs, as well as an overlap with previous findings from DisGeNET, the cell type enrichment and gene ontology analyses indicated considerable divergence between results in humans and mice, indicating possible mechanistic differences between the murine social defeat model and human depression, at least in what concerns the OB. It is plausible to assume that this divergence is at least partially related to the disproportionately greater OB/brain volume in mice compared to humans.

The current study contributes to a better understanding of the cellular and molecular factors associated with MDD, which is required for the design of impactful translational studies, including research on diagnostic or prognostic biomarkers as well as on emerging therapeutics. A growing body of evidence suggests that astrocyte-derived extracellular vesicles can be obtained non-invasively from the serum of MDD patients and inform on the functional state of astrocytes *in vivo* (Xie et al., 2023). Our OB proteomic findings reveal the downregulation of several astrocytic markers such as ALDOC and proteins that are highly expressed in astrocytes such as CD44. The presence of both proteins has been previously confirmed in CSF, serum and extracellular vesicles in peripheral blood (Ampuero et al., 2015; Gomez-Molina et al., 2019; O'Leary and Mechawar, 2021). It remains to be determined if peripheral levels of these proteins

are correlated with astrocytic deficits in one or multiple regions of the CNS and with one or more astrocytic subtypes.

The main limitations of our study were its sample size and the fact that all the OBs were from male donors. It is challenging to collect postmortem OB samples, and particularly samples that are of sufficient quality for proteomics, and this becomes even more difficult by the very low number of OBs collected from female middle-aged depressed suicides over the years. As a result, we were unable to include female samples in a way that would be significantly meaningful while maintaining matched subject groups. Given the distinct male vs female molecular signatures of depression that have been reported in other brain regions, especially in astrocytes and microglia (Maitra et al., 2023), future investigations will need to circumvent these challenges to explore whether the OB is similarly affected in female depressed suicides. Furthermore, while we matched subject covariates as closely as possible across groups, the post-mortem intervals may have influenced protein degradation, phosphorylation and or their relative proportion. Finally, it is noteworthy that we did not investigate the OB of MDD patients who did not die by suicide. Suicidality itself likely poses at least a partly unique neurobiological signature, thus we cannot assume that the proteomic signature we detected is fully representative of all individuals affected by MDD patients (Peng et al., 2023).

Overall, the findings of our study further implicate astrocytes in depression and suicide, using proteomic, phosphoproteomic, and histologic approaches. The consistency of cortico-limbic astrocyte findings in depression research lends support to the notion that this cell type might play a key role in the pathophysiology of the disease. Furthermore, our study raises the possibility that the chronic social defeat stress model of depressive-like behavior might not sufficiently recapitulate the molecular neurobiology of human depression and suicide, at least in the OB.

Understanding the strengths and weaknesses of animal models of depression will help to better position pre-clinical research questions such that their translatability to human depression may be enhanced.

Data availability

The mass spectrometry proteomics data have been deposited to the ProteomeXchange Consortium via the PRIDE partner repository with the dataset identifier PXD045011.
The processed spreadsheets for human proteomics and phosphoproteomics, as well as the mouse proteomics have been provided as Supplementary Tables 7 (human proteomics). Supplementary Table 8 (human phosphoproteomics), and Supplementary Table 9 (mouse proteomics). The cell type marker list for the enrichment analysis has been as Supplementary Table 3 as well.

REFERENCES

Abbink, M.R., Kotah, J.M., Hoeijmakers, L., Mak, A., Yvon-Durocher, G., van der Gaag, B., Lucassen, P.J., Korosi, A., 2020. Characterization of astrocytes throughout life in wildtype and APP/PS1 mice after early-life stress exposure. J. Neuroinflammation 17, 91.

Ampuero, E., Luarte, A., Santibanez, M., Varas-Godoy, M., Toledo, J., Diaz-Veliz, G., Cavada, G., Rubio, F.J., Wyneken, U., 2015. Two Chronic Stress Models Based on Movement Restriction in Rats Respond Selectively to Antidepressant Drugs: Aldolase C As a Potential Biomarker. Int. J. Neuropsychopharmacol. 18, pyv038.

Ardito, F., Giuliani, M., Perrone, D., Troiano, G., Lo Muzio, L., 2017. The crucial role of protein phosphorylation in cell signaling and its use as targeted therapy (Review). Int. J. Mol. Med. 40, 271-280.

Athanassi, A., Dorado Doncel, R., Bath, K.G., Mandairon, N., 2021. Relationship between depression and olfactory sensory function: a review. Chem. Senses 46.

Beck, F., Geiger, J., Gambaryan, S., Solari, F.A., Dell'Aica, M., Loroch, S., Mattheij, N.J., Mindukshev, I., Potz, O., Jurk, K., Burkhart, J.M., Fufezan, C., Heemskerk, J.W., Walter, U., Zahedi, R.P., Sickmann, A., 2017. Temporal quantitative phosphoproteomics of ADP stimulation reveals novel central nodes in platelet activation and inhibition. Blood 129, e1-e12.

Bonnefil, V., Dietz, K., Amatruda, M., Wentling, M., Aubry, A.V., Dupree, J.L., Temple, G., Park, H.J., Burghardt, N.S., Casaccia, P., Liu, J., 2019. Region-specific myelin

differences define behavioral consequences of chronic social defeat stress in mice. Elife 8.
Burkhart, J.M., Schumbrutzki, C., Wortelkamp, S., Sickmann, A., Zahedi, R.P., 2012. Systematic and quantitative comparison of digest efficiency and specificity reveals the impact of trypsin quality on MS-based proteomics. J. Proteomics 75, 1454-1462.
Codeluppi, S.A., Chatterjee, D., Prevot, T.D., Bansal, Y., Misquitta, K.A., Sibille, E., Banasr, M., 2021. Chronic Stress Alters Astrocyte Morphology in Mouse Prefrontal Cortex. Int. J. Neuropsychopharmacol. 24, 842-853.
Croy, I., Hummel, T., 2017. Olfaction as a marker for depression. J. Neurol. 264, 631-638.
Croy, I., Negoias, S., Novakova, L., Landis, B.N., Hummel, T., 2012. Learning about the functions of the olfactory system from people without a sense of smell. PLoS One 7, e33365.
Du Preez, A., Onorato, D., Eiben, I., Musaelyan, K., Egeland, M., Zunszain, P.A., Fernandes, C., Thuret, S., Pariante, C.M., 2021. Chronic stress followed by social isolation promotes depressive-like behaviour, alters microglial and astrocyte biology and reduces hippocampal neurogenesis in male mice. Brain. Behav. Immun. 91, 24-47.
Dumais, A., Lesage, A.D., Lalovic, A., Seguin, M., Tousignant, M., Chawky, N., Turecki, G., 2005. Is violent method of suicide a behavioral marker of lifetime aggression? Am. J. Psychiatry 162, 1375-1378.
Duman, R.S., Aghajanian, G.K., Sanacora, G., Krystal, J.H., 2016. Synaptic plasticity and depression: new insights from stress and rapid-acting antidepressants. Nat. Med. 22, 238-249.
Golden, S.A., Covington, H.E., 3rd, Berton, O., Russo, S.J., 2011. A standardized protocol for repeated social defeat stress in mice. Nat. Protoc. 6, 1183-1191.
Gomez-Molina, C., Sandoval, M., Henzi, R., Ramirez, J.P., Varas-Godoy, M., Luarte, A., Lafourcade, C.A., Lopez-Verrilli, A., Smalla, K.H., Kaehne, T., Wyneken, U., 2019. Small Extracellular Vesicles in Rat Serum Contain Astrocyte-Derived Protein Biomarkers of Repetitive Stress. Int. J. Neuropsychopharmacol. 22, 232-246.
Gonczarowska-Jorge, H., Loroch, S., Dell'Aica, M., Sickmann, A., Roos, A., Zahedi, R.P., 2017. Quantifying missing (phospho)proteome regions with the broad-specificity protease subtilisin. Anal. Chem. 89, 13137-13145.
Holmes, S.E., Scheinost, D., Finnema, S.J., Naganawa, M., Davis, M.T., DellaGioia, N., Nabulsi, N., Matuskey, D., Angarita, G.A., Pietrzak, R.H., Duman, R.S., Sanacora, G., Krystal, J.H., Carson, R.E., Esterlis, I., 2019. Lower synaptic density is associated with depression severity and network alterations. Nat Commun 10, 1529.
Huang, A.Y., Woo, J., Sardar, D., Lozzi, B., Bosquez Huerta, N.A., Lin, C.J., Felice, D., Jain, A., Paulucci-Holthauzen, A., Deneen, B., 2020. Region-Specific Transcriptional Control of Astrocyte Function Oversees Local Circuit Activities. Neuron 106, 992-1008 e1009.
Jahn, O., Tenzer, S., Werner, H.B., 2009. Myelin proteomics: molecular anatomy of an insulating sheath. Mol. Neurobiol. 40, 55-72.
Kelly, J.P., Wrynn, A.S., Leonard, B.E., 1997. The olfactory bulbectomized rat as a model of depression: an update. Pharmacol. Ther. 74, 299-316.
Kohli, P., Soler, Z.M., Nguyen, S.A., Muus, J.S., Schlosser, R.J., 2016. The Association Between Olfaction and Depression: A Systematic Review. Chem. Senses 41, 479-486.
Kokkosis, A.G., Madeira, M.M., Mullahy, M.R., Tsirka, S.E., 2022. Chronic stress disrupts the homeostasis and progeny progression of oligodendroglial lineage cells, associating

immune oligodendrocytes with prefrontal cortex hypomyelination. Mol. Psychiatry 27, 2833-2848.
Liu, J., Dietz, K., DeLoyht, J.M., Pedre, X., Kelkar, D., Kaur, J., Vialou, V., Lobo, M.K., Dietz, D.M., Nestler, E.J., Dupree, J., Casaccia, P., 2012. Impaired adult myelination in the prefrontal cortex of socially isolated mice. Nat. Neurosci. 15, 1621-1623.
Lombion-Pouthier, S., Vandel, P., Nezelof, S., Haffen, E., Millot, J.L., 2006. Odor perception in patients with mood disorders. J. Affect. Disord. 90, 187-191.
Maheu, M.E., Devorak, J., Freibauer, A., Davoli, M.A., Turecki, G., Mechawar, N., 2015. Increased doublecortin (DCX) expression and incidence of DCX-immunoreactive multipolar cells in the subventricular zone-olfactory bulb system of suicides. Front. Neuroanat. 9, 74.
Maitra, M., Mitsuhashi, H., Rahimian, R., Chawla, A., Yang, J., Fiori, L.M., Davoli, M.A., Perlman, K., Aouabed, Z., Mash, D.C., Suderman, M., Mechawar, N., Turecki, G., Nagy, C., 2023. Cell type specific transcriptomic differences in depression show similar patterns between males and females but implicate distinct cell types and genes. Nat Commun 14, 2912.
Makinodan, M., Rosen, K.M., Ito, S., Corfas, G., 2012. A critical period for social experience-dependent oligodendrocyte maturation and myelination. Science 337, 1357-1360.
Martins-de-Souza, D., Guest, P.C., Vanattou-Saifoudine, N., Rahmoune, H., Bahn, S., 2012. Phosphoproteomic differences in major depressive disorder postmortem brains indicate effects on synaptic function. Eur. Arch. Psychiatry Clin. Neurosci. 262, 657-666.
McKenzie, A.T., Wang, M., Hauberg, M.E., Fullard, J.F., Kozlenkov, A., Keenan, A., Hurd, Y.L., Dracheva, S., Casaccia, P., Roussos, P., Zhang, B., 2018. Brain cell type specific gene expression and co-expression network architectures. Sci. Rep. 8, 8868.
Mechawar, N., Saghatelyan, A., Grailhe, R., Scoriels, L., Gheusi, G., Gabellec, M.M., Lledo, P.M., Changeux, J.P., 2004. Nicotinic receptors regulate the survival of newborn neurons in the adult olfactory bulb. Proc. Natl. Acad. Sci. U. S. A. 101, 9822-9826.
Milardi, D., Cacciola, A., Calamuneri, A., Ghilardi, M.F., Caminiti, F., Cascio, F., Andronaco, V., Anastasi, G., Mormina, E., Arrigo, A., Bruschetta, D., Quartarone, A., 2017. The Olfactory System Revealed: Non-Invasive Mapping by using Constrained Spherical Deconvolution Tractography in Healthy Humans. Front. Neuroanat. 11, 32.
Nagy, C., Maitra, M., Tanti, A., Suderman, M., Theroux, J.F., Davoli, M.A., Perlman, K., Yerko, V., Wang, Y.C., Tripathy, S.J., Pavlidis, P., Mechawar, N., Ragoussis, J., Turecki, G., 2020. Single-nucleus transcriptomics of the prefrontal cortex in major depressive disorder implicates oligodendrocyte precursor cells and excitatory neurons. Nat. Neurosci. 23, 771-781.
Navarro, P., Trevisan-Herraz, M., Bonzon-Kulichenko, E., Nunez, E., Martinez-Acedo, P., Perez-Hernandez, D., Jorge, I., Mesa, R., Calvo, E., Carrascal, M., Hernaez, M.L., Garcia, F., Barcena, J.A., Ashman, K., Abian, J., Gil, C., Redondo, J.M., Vazquez, J., 2014. General statistical framework for quantitative proteomics by stable isotope labeling. J. Proteome Res. 13, 1234-1247.
Negoias, S., Croy, I., Gerber, J., Puschmann, S., Petrowski, K., Joraschky, P., Hummel, T., 2010. Reduced olfactory bulb volume and olfactory sensitivity in patients with acute major depression. Neuroscience 169, 415-421.

O'Leary, L.A., Belliveau, C., Davoli, M.A., Ma, J.C., Tanti, A., Turecki, G., Mechawar, N., 2021. Widespread Decrease of Cerebral Vimentin-Immunoreactive Astrocytes in Depressed Suicides. Front Psychiatry 12, 640963.

O'Leary, L.A., Mechawar, N., 2021. Implication of cerebral astrocytes in major depression: A review of fine neuroanatomical evidence in humans. Glia 69, 2077-2099.

Pause, B.M., Miranda, A., Goder, R., Aldenhoff, J.B., Ferstl, R., 2001. Reduced olfactory performance in patients with major depression. J. Psychiatr. Res. 35, 271-277.

Pellerin, L., Magistretti, P.J., 1994. Glutamate uptake into astrocytes stimulates aerobic glycolysis: a mechanism coupling neuronal activity to glucose utilization. Proc. Natl. Acad. Sci. U. S. A. 91, 10625-10629.

Peng, S., Zhou, Y., Xiong, L., Wang, Q., 2023. Identification of novel targets and pathways to distinguish suicide dependent or independent on depression diagnosis. Sci. Rep. 13, 2488.

Perez-Catalan, N.A., Doe, C.Q., Ackerman, S.D., 2021. The role of astrocyte-mediated plasticity in neural circuit development and function. Neural Dev 16, 1.

Qiu, Y., Wang, J., Lei, J., Roeder, K., 2021. Identification of cell-type-specific marker genes from co-expression patterns in tissue samples. Bioinformatics 37, 3228-3234.

Rahimian, R., Perlman, K., Canonne, C., Mechawar, N., 2022. Targeting microglia-oligodendrocyte crosstalk in neurodegenerative and psychiatric disorders. Drug Discov Today 27, 2562-2573.

Rajkowska, G., Hughes, J., Stockmeier, C.A., Javier Miguel-Hidalgo, J., Maciag, D., 2013. Coverage of blood vessels by astrocytic endfeet is reduced in major depressive disorder. Biol. Psychiatry 73, 613-621.

Rajkowska, G., Miguel-Hidalgo, J.J., 2007. Gliogenesis and glial pathology in depression. CNS Neurol. Disord. Drug Targets 6, 219-233.

Reemst, K., Kracht, L., Kotah, J.M., Rahimian, R., van Irsen, A.A.S., Congrains Sotomayor, G., Verboon, L.N., Brouwer, N., Simard, S., Turecki, G., Mechawar, N., Kooistra, S.M., Eggen, B.J.L., Korosi, A., 2022. Early-life stress lastingly impacts microglial transcriptome and function under basal and immune-challenged conditions. Transl Psychiatry 12, 507.

Ren, F., Guo, R., 2021. Synaptic Microenvironment in Depressive Disorder: Insights from Synaptic Plasticity. Neuropsychiatr. Dis. Treat. 17, 157-165.

Rothhammer, V., Kenison, J.E., Tjon, E., Takenaka, M.C., de Lima, K.A., Borucki, D.M., Chao, C.C., Wilz, A., Blain, M., Healy, L., Antel, J., Quintana, F.J., 2017. Sphingosine 1-phosphate receptor modulation suppresses pathogenic astrocyte activation and chronic progressive CNS inflammation. Proc. Natl. Acad. Sci. U. S. A. 114, 2012-2017.

Rottstaedt, F., Weidner, K., Strauss, T., Schellong, J., Kitzler, H., Wolff-Stephan, S., Hummel, T., Croy, I., 2018. Size matters - The olfactory bulb as a marker for depression. J. Affect. Disord. 229, 193-198.

Rurak, G.M., Woodside, B., Aguilar-Valles, A., Salmaso, N., 2021. Astroglial cells as neuroendocrine targets in forebrain development: Implications for sex differences in psychiatric disease. Front. Neuroendocrinol. 60, 100897.

Scarpa, J.R., Fatma, M., Loh, Y.E., Traore, S.R., Stefan, T., Chen, T.H., Nestler, E.J., Labonte, B., 2020. Shared Transcriptional Signatures in Major Depressive Disorder and Mouse Chronic Stress Models. Biol. Psychiatry 88, 159-168.

Simard, S., Coppola, G., Rudyk, C.A., Hayley, S., McQuaid, R.J., Salmaso, N., 2018. Profiling changes in cortical astroglial cells following chronic stress. Neuropsychopharmacology 43, 1961-1971.

Song, C., Leonard, B.E., 2005. The olfactory bulbectomised rat as a model of depression. Neurosci. Biobehav. Rev. 29, 627-647.

Sun, J., Bronk, P., Liu, X., Han, W., Sudhof, T.C., 2006. Synapsins regulate use-dependent synaptic plasticity in the calyx of Held by a Ca2+/calmodulin-dependent pathway. Proc. Natl. Acad. Sci. U. S. A. 103, 2880-2885.

Takahashi, T., Nishikawa, Y., Yucel, M., Whittle, S., Lorenzetti, V., Walterfang, M., Sasabayashi, D., Suzuki, M., Pantelis, C., Allen, N.B., 2016. Olfactory sulcus morphology in patients with current and past major depression. Psychiatry Res Neuroimaging 255, 60-65.

Tanti, A., Belliveau, C., Nagy, C., Maitra, M., Denux, F., Perlman, K., Chen, F., Mpai, R., Canonne, C., Théberge, S., McFarquhar, A., Davoli, M.A., Belzung, C., Turecki, G., Mechawar, N., 2022. Child abuse associates with increased recruitment of perineuronal nets in the ventromedial prefrontal cortex: a possible implication of oligodendrocyte progenitor cells. Mol. Psychiatry 27, 1552-1561.

Tchieu, J., Calder, E.L., Guttikonda, S.R., Gutzwiller, E.M., Aromolaran, K.A., Steinbeck, J.A., Goldstein, P.A., Studer, L., 2019. NFIA is a gliogenic switch enabling rapid derivation of functional human astrocytes from pluripotent stem cells. Nat. Biotechnol. 37, 267-275.

Torres-Platas, S.G., Nagy, C., Wakid, M., Turecki, G., Mechawar, N., 2016. Glial fibrillary acidic protein is differentially expressed across cortical and subcortical regions in healthy brains and downregulated in the thalamus and caudate nucleus of depressed suicides. Mol. Psychiatry 21, 509-515.

Ung, K., Huang, T.W., Lozzi, B., Woo, J., Hanson, E., Pekarek, B., Tepe, B., Sardar, D., Cheng, Y.T., Liu, G., Deneen, B., Arenkiel, B.R., 2021. Olfactory bulb astrocytes mediate sensory circuit processing through Sox9 in the mouse brain. Nat Commun 12, 5230.

Ventorp, F., Barzilay, R., Erhardt, S., Samuelsson, M., Traskman-Bendz, L., Janelidze, S., Weizman, A., Offen, D., Brundin, L., 2016. The CD44 ligand hyaluronic acid is elevated in the cerebrospinal fluid of suicide attempters and is associated with increased blood-brain barrier permeability. J. Affect. Disord. 193, 349-354.

Waller, R., Murphy, M., Garwood, C.J., Jennings, L., Heath, P.R., Chambers, A., Matthews, F.E., Brayne, C., Ince, P.G., Wharton, S.B., Simpson, J.E., Cognitive, F., Ageing Neuropathology Study, G., 2018. Metallothionein-I/II expression associates with the astrocyte DNA damage response and not Alzheimer-type pathology in the aging brain. Glia 66, 2316-2323.

Xie, X.H., Lai, W.T., Xu, S.X., Di Forti, M., Zhang, J.Y., Chen, M.M., Yao, L.H., Wang, P., Hao, K.K., Rong, H., 2023. Hyper-inflammation of astrocytes in patients of major depressive disorder: Evidence from serum astrocyte-derived extracellular vesicles. Brain. Behav. Immun. 109, 51-62.

Xiong, W., Cao, X., Zeng, Y., Qin, X., Zhu, M., Ren, J., Wu, Z., Huang, Q., Zhang, Y., Wang, M., Chen, L., Turecki, G., Mechawar, N., Chen, W., Yi, G., Zhu, X., 2019. Astrocytic epoxyeicosatrienoic acid signaling in the medial prefrontal cortex modulates depressive-like behaviors. J. Neurosci. 39, 4606-4623.

Zhao, J., Verwer, R.W., van Wamelen, D.J., Qi, X.R., Gao, S.F., Lucassen, P.J., Swaab, D.F., 2016. Prefrontal changes in the glutamate-glutamine cycle and neuronal/glial glutamate transporters in depression with and without suicide. J. Psychiatr. Res. 82, 8-15.

AUTHOR CONTRIBUTIONS

NM conceptualized the study. RR prepared samples for proteomic experiments and performed all FISH validations. RR, KP and NM wrote the manuscript and prepared the figures. KP performed the bioinformatic analyses for the proteomic and phosphoproteomic data. RM and MAD conducted histological work. GF and LP performed animal behavioral tests. GF extracted mouse OBs and analyzed the behavioral tasks. CH contributed to the FISH analysis. VR, RPZ and CB performed proteomic and phosphoproteomic experiments. NM, BG, CN and GT supervised the project. All authors read, contributed to, and agreed with the final version of the manuscript.

ACKNOWLEDGMENTS

This study was funded by an ERA NET Neuron grant and a CIHR Project grant to N.M. R.R. and G.F. received fellowships and K.P. a scholarship from the FRQ-S. K.P. currently holds a CIHR doctoral scholarship and R.M. a scholarship from the Botswana government. The Douglas-Bell Canada Brain Bank is supported in part by platform support grants from the Réseau Québécois sur le Suicide, les Troubles de l'Humeur et les Troubles Associés (FRQ-S), Healthy Brains for Healthy Lives (CFREF), and Brain Canada. This study used the services of the Molecular and Cellular Microscopy Platform (MCMP) at the Douglas Research Centre.

This work was also supported by funding to CHB from Genome Canada's Genomics Technology Platform (264PRO). CHB is also grateful for support from the Segal McGill Chair in Molecular Oncology at McGill University (Montreal, Quebec, Canada) for support from the Terry Fox Research Institute, the Warren Y. Soper Charitable Trust, and the Alvin Segal Family Foundation to the Jewish General Hospital (Montreal, Quebec, Canada).

This work was done under the auspices of a Memorandum of Understanding between McGill and the U.S. National Cancer Institute's International Cancer Proteogenome Consortium (ICPC). ICPC encourages international cooperation among institutions and nations in proteogenomic cancer research in which proteogenomic datasets are made available to the public. This work was also done in collaboration with the U.S. National Cancer Institute's Clinical Proteomic Tumor Analysis Consortium (CPTAC).

Lastly, the authors wish to thank the donors and their families for their invaluable gift.

COMPETING INTERESTS

CHB is the CSO of MRM Proteomics Inc., and the VP of Proteomics at Molecular You. RPZ is CEO of MRM Proteomics. The remaining authors declare no conflict of interest.

ADDITIONAL INFORMATION

Supplementary information

Figure legends

Figure 1. Human OB proteomics reveal enrichment in astrocyte-specific differentially expressed proteins in depressed suicides. (**A**) Volcano plot with log base 2 abundance ratio between depressed suicides and controls on the x-axis and the $-\log_{10}$(p-value) on the y-axis. Each dot represents a protein, and they are colored by direction of regulation with downregulation in pink and upregulation in turquoise. The log base 2 abundance ratio cutoff is |2.5| for visualization purposes and the p-value is cutoff is $-\log_{10}(0.05)$. (**B**) Bar plot with $-\log_{10}$(false discovery rate) on the x-axis and KEGG term on the axis. This plot shows the over enriched KEGG terms in the list of differentially expressed proteins between depressed suicides and controls. The bars are colored by the strength of the enrichment of the term. (C) Ridge plot with the enrichment of the

gene ontology (GO) terms on the x-axis, and each GO biological process listed on the x-axis. This plot shows the over enriched GO terms in the list of differentially expressed proteins between depressed suicides and controls. The ridges are colored by adjusted p-value of the enrichment tests as demonstrated by the color bar. (**D**) Table of overlap of proteins in list of differentially expressed proteins and genes found in the DisGeNET database. Proteins are listed in descending order by log base 2-fold change between depressed suicides and controls. Proteins with positive fold change values are colored in pink and negative fold change values are colored in blue. (**E**) Bar plot showing cell type enrichment scores of differentially expressed proteins. The x-axis shows the broad cell types of the brain, and the y-axis shows the $-\log_{10}$(p-value), where the p-value refers to the enrichment p-value from hypergeometric tests. The dotted line refers to the significance cutoff which is $-\log_{10}(0.05)$. Only the astrocytes surpass this significance threshold.

Figure 2. Translational deregulation of canonical astrocytic markers in depressed suicide OBs. (**A**) Heat map illustrating differentially expressed canonical astrocytic markers in OBs from CTRL individuals as opposed to those from depressed suicide subjects. GFAP and SLC1A3 proteins were significantly downregulated in MDD OBs (respectively, p = 0.0013 and p = 0.017), while ALDOC, NFIA, ALDH1L1, and GJA1 showed a downregulation trend. (**B**) Left: Representative microphotographs of FISH experiments on CTRL and MDD OBs using ALDH1L1 probe. Right: percentage of ALDH1L1$^+$ cells, p = 0.1406. **C**-**F**) Left: Representative microphotographs of FISH experiments on CTRL and MDD OBs using ALDH1L1 probe along with (**C**) ALDOC, (**D**) GJA1, (**E**) NFIA, or (**F**) SLC1A3 probes. Right: percentage of double

positive astrocytes over the total number of astrocytes (ALDH1L1^{+} cells). (**C**) p = 0.0272; (**D**) p = 0.031; (**E**) p = 0.007; (F) p = 0.024. (**B**-**F**) CTRL: n = 3; MDD: n = 5; scale bars: 20µm.

Figure 3. Human OB differential phosphoproteomics in depressed suicides. (**A**) Volcano plot with log base 2 abundance ratio between depressed suicides and controls on the x-axis and the -$\log_{10}$(p-value) on the y-axis. Each dot represents a protein that showed significant phosphopeptide differential regulation between depressed suicides and controls, and the points are colored by direction of the regulation of the abundance of the phosphopeptide modification with downregulation in pink and upregulation in turquoise. The log base 2 abundance ratio cutoff is |3| for visualization purposes and the p-value is cutoff is -$\log_{10}$(0.05). (**B**) Ridge plot with the enrichment of the gene ontology (GO) terms on the x-axis, and each GO biological process listed on the x-axis. This plot shows the over enriched GO terms in the list of differentially expressed proteins between depressed suicides and controls. The ridges are colored by adjusted p-value of the enrichment tests as demonstrated by the color bar. (**C**) Table of overlap of proteins in list of proteins with differentially expressed phosphopeptide and genes found in the DisGeNET database. Proteins are listed in descending order by log base 2-fold change between depressed suicides and controls. Abundance of the differentially expressed phosphopeptide modification for the protein between depressed suicides and controls is represented by log base 2-fold change, phosphopeptide with positive fold change values are colored in pink and negative fold change values are colored in blue. In cases where there were multiple phosphopeptide regulation for a given protein, the average fold change across all modifications was used. (**D**) Bar plot showing cell type enrichment scores of differentially expressed proteins. The x-axis shows the broad cell types of the brain and the y-axis shows the -$\log_{10}$(p-value), where the p-value refers to the

enrichment p-value from hypergeometric tests. The dotted line refers to the significance cutoff which is $-\log_{10}(0.05)$. Only the neurons and astrocytes surpass this significance threshold.

Figure 4. OB proteomics of social defeat stress mice do not recapitulate human OB proteomics of depressed suicides. Plots **A**-**C** demonstrate the behavioral tests conducted on control and socially defeated mice, CTRL, n = 6; SD, n = 8. (**A**) $p = 0.002$; (**B**) $p = 0.012$; (**C**) $p = 0.012$. (**D**) Volcano plot with log base 2 abundance ratio between depressed suicides and controls on the x-axis and the $-\log_{10}$(p-value) on the y-axis. Each dot represents a protein, and they are colored by direction of regulation with downregulation in pink and upregulation in turquoise. The log base 2 abundance ratio cutoff is |2.5| for visualization purposes and the p-value is cutoff is $-\log_{10}(0.05)$. (**E**) Ridge plot with the enrichment of the gene ontology (GO) terms on the x-axis, and each GO biological process listed on the x-axis. This plot shows the over enriched GO terms in the list of differentially expressed proteins between depressed suicides and controls. The ridges are colored by adjusted p-value of the enrichment tests as demonstrated by the color bar. (**F**) Table of overlap of proteins in list of differentially expressed proteins and genes found in the DisGeNET database. Proteins are listed in descending order by log base 2-fold change between depressed suicides and controls. Proteins with positive fold change values are colored in pink and negative fold change values are colored in blue. (**G**) Bar plot showing cell type enrichment scores of differentially expressed proteins. The x-axis shows the broad cell types of the brain, and the y-axis shows the $-\log_{10}$(p-value), where the p-value refers to the enrichment p-value from hypergeometric tests. The dotted line refers to the significance cutoff which is $-\log_{10}(0.05)$. Only the OL-lineage cells surpass this significance threshold.

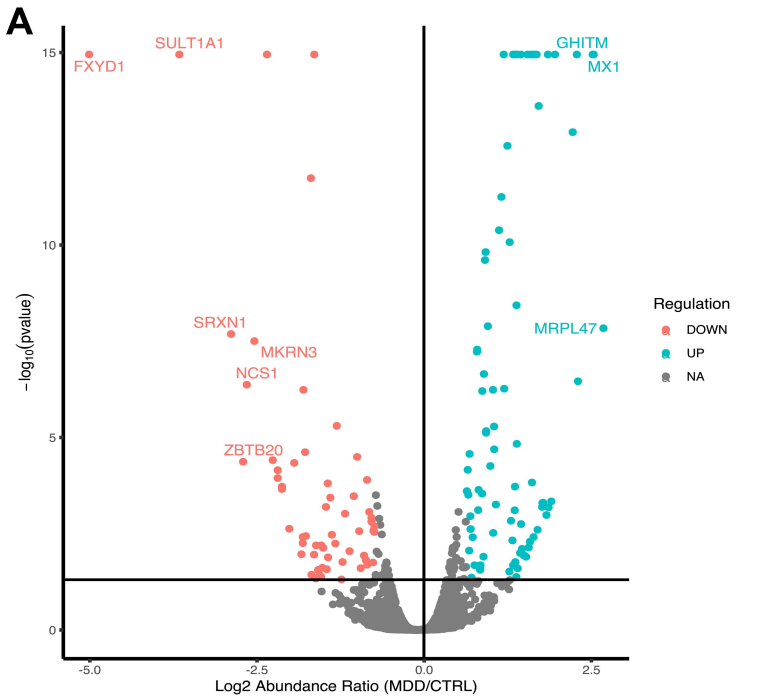

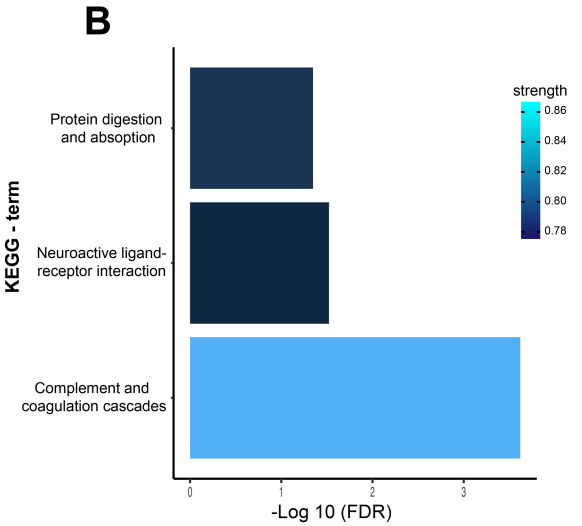

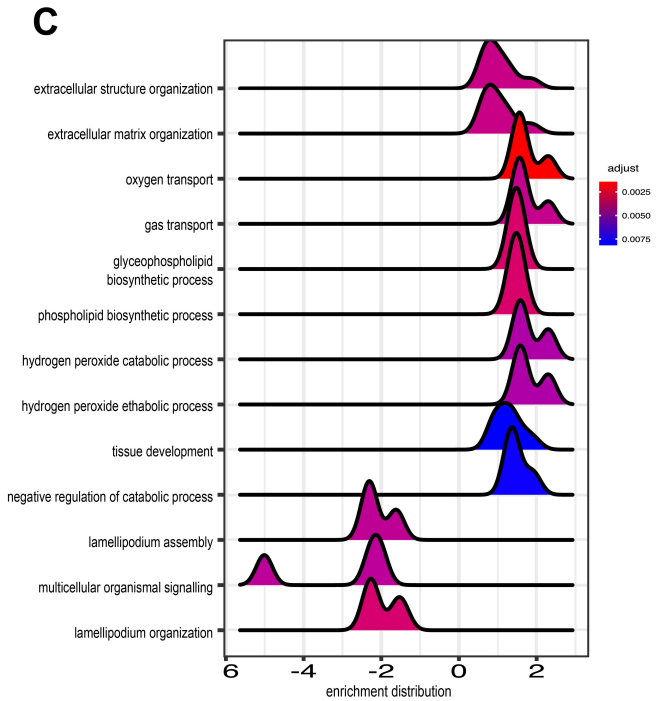

D

Name	log_2FC MDD/CTRL
GSTM1	2.28
GRM3	1.69
SIGMAR1	1.45
APOA1	1.39
APOA2	1.38
TTR	1.33
HLA-C	1.07
PLG	1.05
OGN	1.03
GC	0.95
FBN1	0.93
BGN	0.89
CFH	0.81
ALB	0.79
CFB	0.55
CAT	0.47
NT5E	0.47
CALD1	0.45
C3	0.43
ACTG2	0.41
CA2	0.37
DBI	-0.54
SLC1A3	-0.56
GFAP	-0.67
MAP6	-0.68
CTNNB1	-0.70
NQO1	-0.74
S100A1	-0.79
CTNND2	-0.82
WASF3	-1.44
GALC	-1.62
NCS1	-2.65
ZBTB20	-2.71
SULT1A1	-3.66

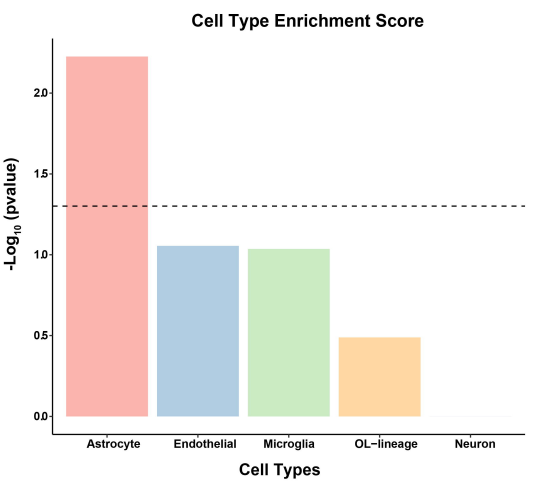

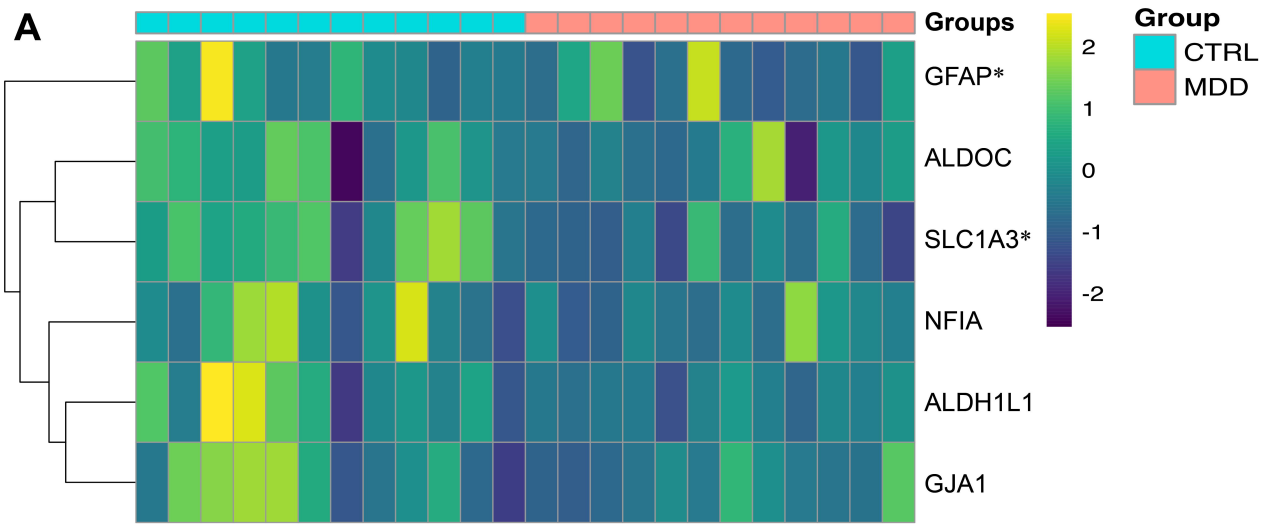
A
Groups
GFAP*
ALDOC
SLC1A3*
NFIA
ALDH1L1
GJA1
2
1
0
-1
-2
Group
CTRL
MDD

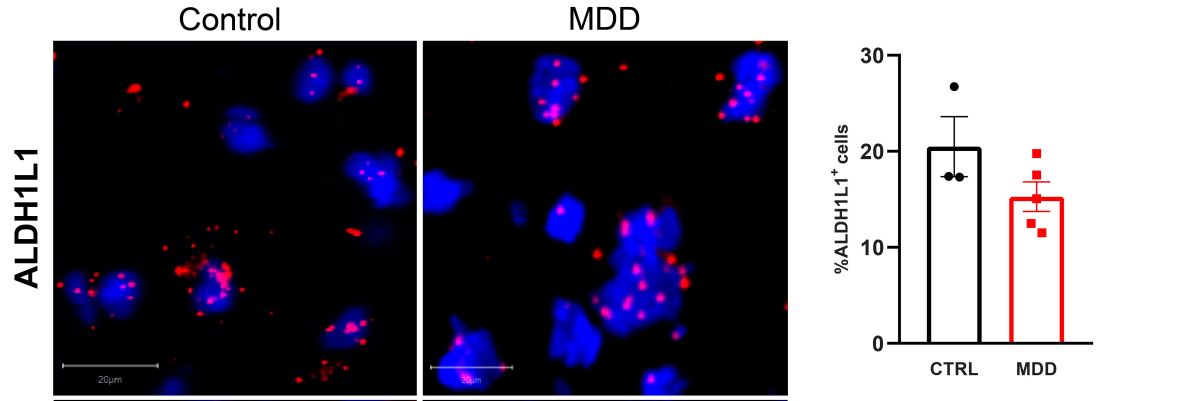
Control
MDD
B
ALDH1L1
%ALDH1L1+ cells
30
20
10
0
CTRL
MDD

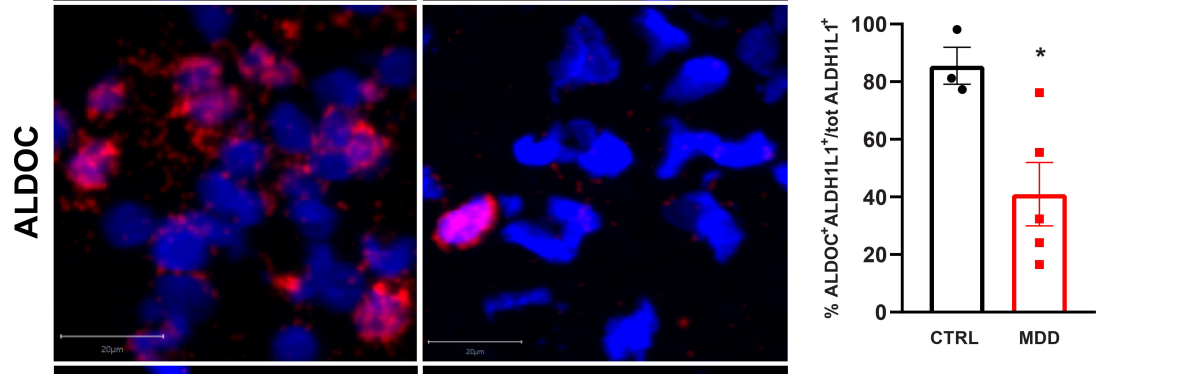
C
ALDOC
% ALDOC+ALDH1L1+/tot ALDH1L1+
100
80
60
40
20
0
*
CTRL
MDD

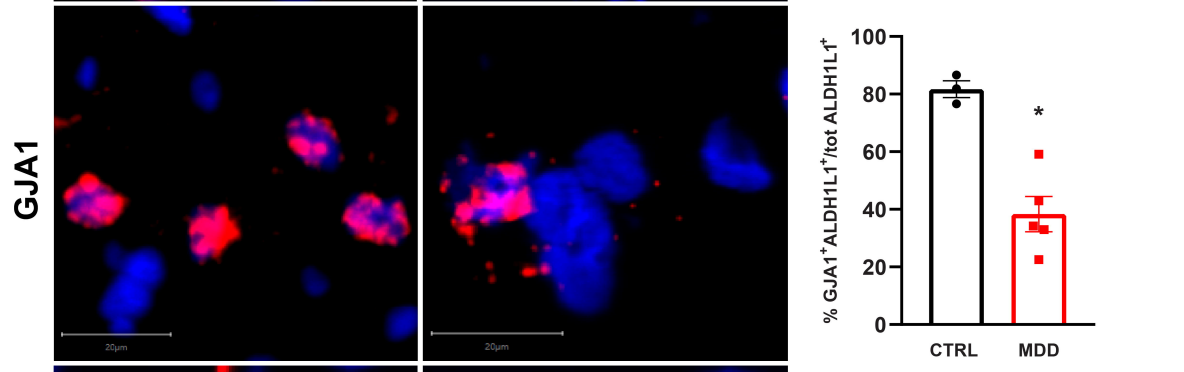
D
GJA1
% GJA1+ALDH1L1+/tot ALDH1L1+
100
80
60
40
20
0
*
CTRL
MDD

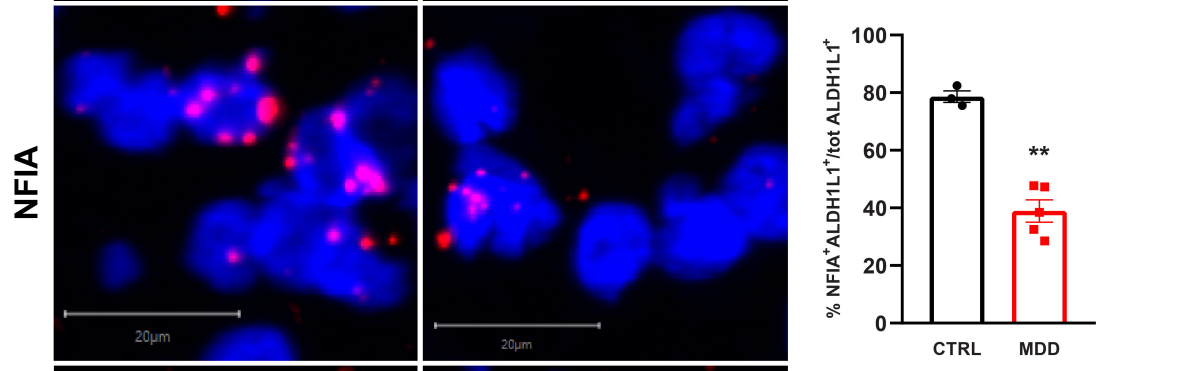
E
NFIA
20µm
20µm
% NFIA+ALDH1L1+/tot ALDH1L1+
100
80
60
40
20
0
**
CTRL
MDD

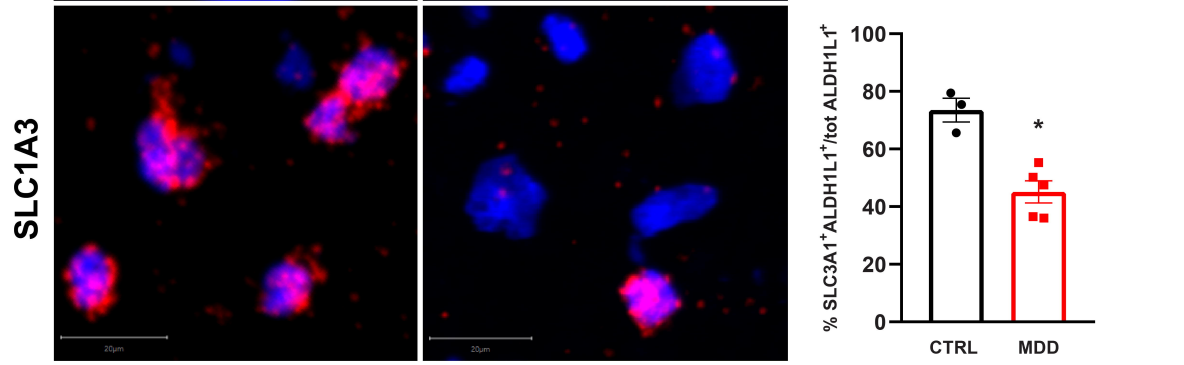
F
SLC1A3
% SLC3A1+ALDH1L1+/tot ALDH1L1+
100
80
60
40
20
0
*
CTRL
MDD

A

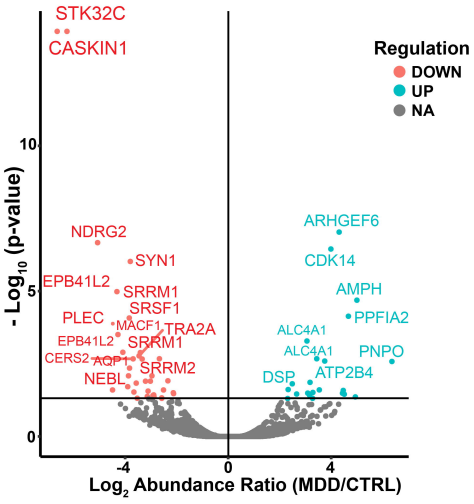

B

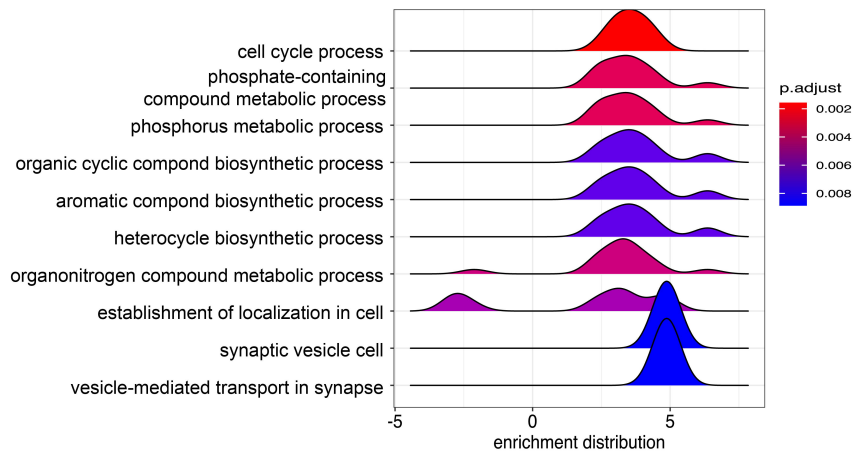

C

Name	log_2FC MDD/CTRL
SYN2	4.94
HSP90AB1	2.66
GFAP	-2.12
NEFM	-2.34
MBP	-2.51
SGIP1	-2.88
DPYSL2	-3.57
SYN1	-3.8
NDRG2	-5.07
STK32C	-6.26

D

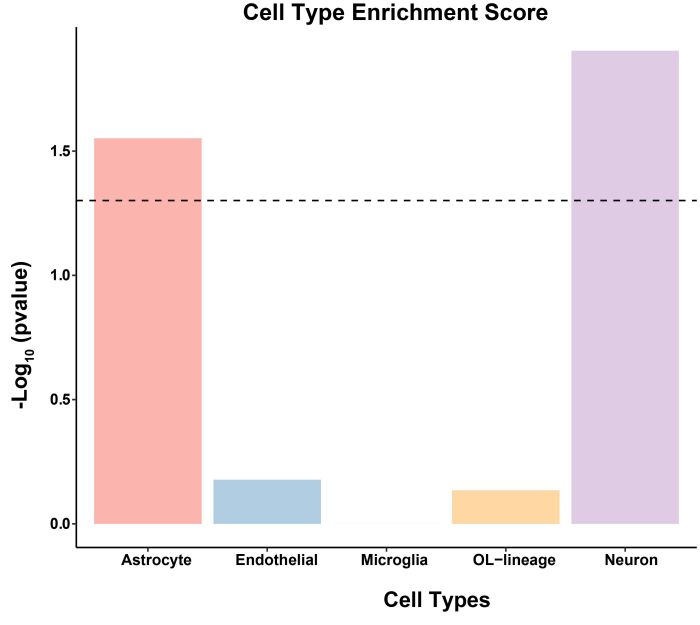

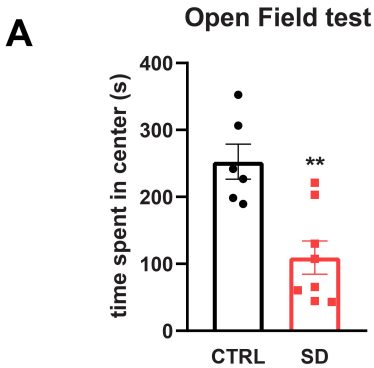

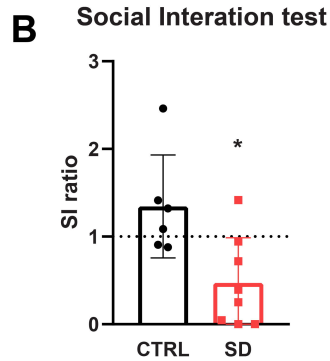

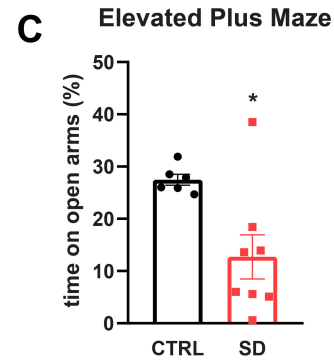

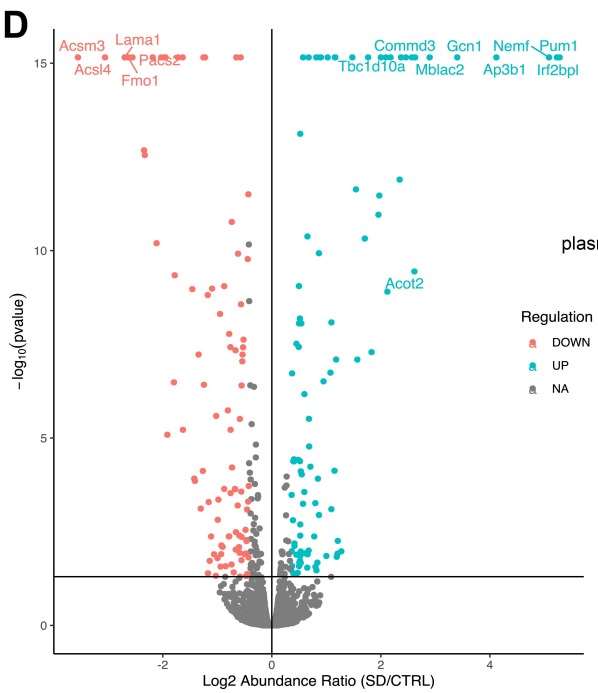

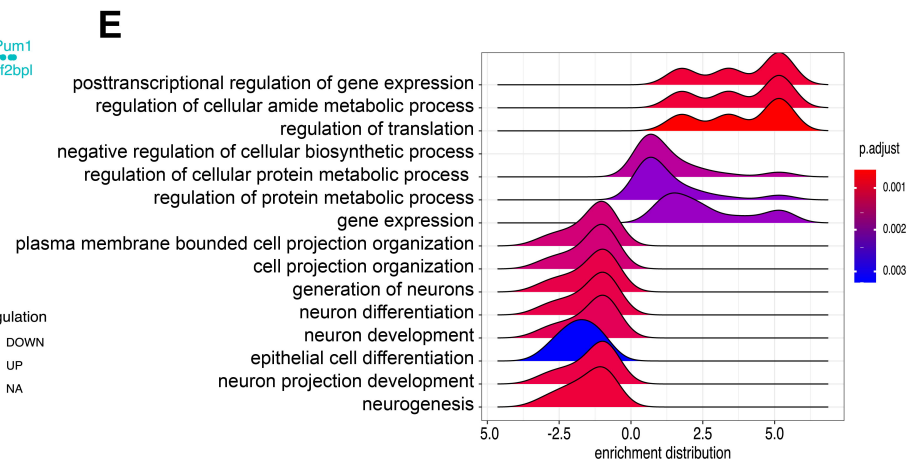

F
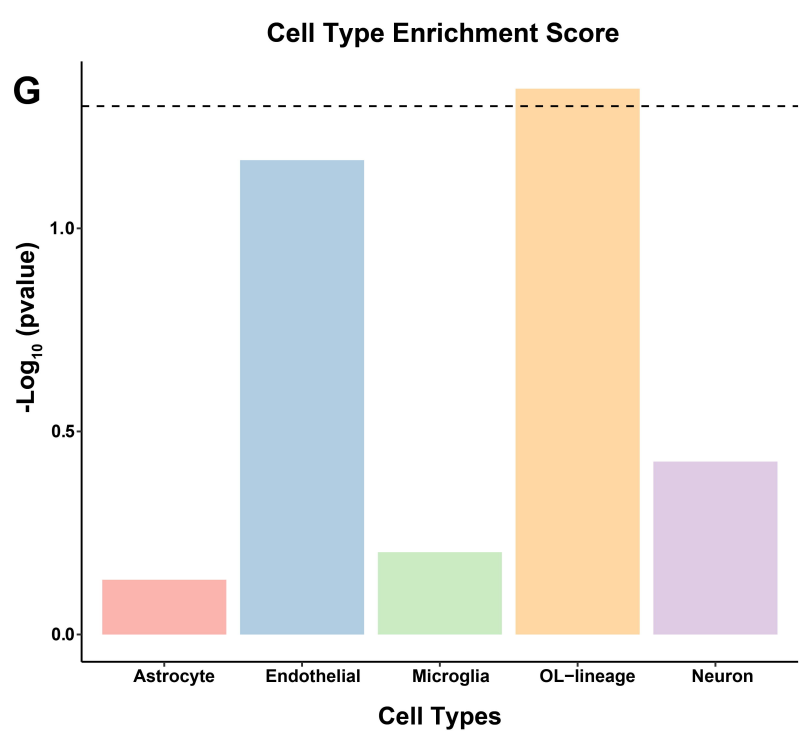
Name	log_2FC SD/CTRL
Commd3	2.63
Apoa1	1.48
Pten	0.68
Hmgb1	0.68
Hdac6	0.66
Ncs1	0.65
Alb	0.57
Ntrk2	0.55
Nrp1	0.52
Nans	0.52
Atg7	0.50
Hspa2	0.50
Aimp2	0.49
Cat	0.42
Sf3b1	0.39
Rida	0.27
Th	0.19
Plp1	0.18
Nqo1	0.17
Nefm	0.16
Actb	-0.22
Ctnnb1	-0.26
Actg1	-0.31
Gja1	-0.37
Nrgn	-0.39
Msra	-0.39
Ptgds	-0.59
Sort1	-0.76
Cit	-0.76
Nol3	-0.87
Pam	-0.93
Ndel1	-0.95
Vgf	-1.02
Pcmtd1	-1.42
Acsl4	-3.06